CrystEngComm

Accepted Manuscript

ROYAL SOCIETY OF CHEMISTRY

www.rsc.org/crystengcomm

UO_2^{2+}-amino hybrid materials: Structural variation and photocatalysis properties

Xue-Ting Xu[1], Ya-Nan Hou[1], Si-Yue Wei[1], Xiao-Xi Zhang[1], Feng-Ying Bai[2], Li-Xian Sun[3], Zhan Shi[4], Yong-Heng Xing[1]*

[1] College of Chemistry and Chemical engineering, Liaoning Normal University, Huanghe Road 850[#], Dalian City, 116029, P.R. China.

[2] College of Life Science, Liaoning Normal University, Dalian 11602, P.R. China

[3] Guangxi Key Laboratory of Information Materials, Guilin University of Electronic Technology, Guilin 541004, P.R. China

[4] State Key Laboratory of Inorganic Synthesis and Preparative Chemistry, College of Chemistry, Jilin University, Changchun 130012, P.R. China

*e-mail: xingyongheng2000@163.com tel: 0411-82156987

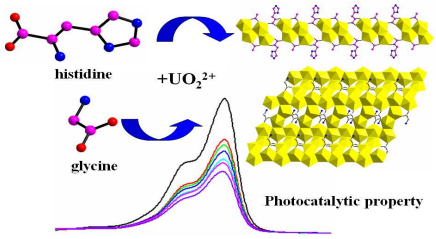

We have synthesized four new uranyl complexes, their photoluminescent characterization and photocatalytic properties were studied in detail.

FULL PAPER

UO_2^{2+}-amino hybrid materials: Structural variation and photocatalysis properties

Xue-Ting Xu[1], Ya-Nan Hou[1], Si-Yue Wei[1], Xiao-Xi Zhang[1], Feng-Ying Bai[2], Li-Xian Sun[3], Zhan Shi[4], Yong-Heng Xing[1]*

[1] College of Chemistry and Chemical engineering, Liaoning Normal University, Huanghe Road 850#, Dalian City, 116029, P.R. China.

[2] College of Life Science, Liaoning Normal University, Dalian 11602, P.R. China

[3] Guangxi Key Laboratory of Information Materials, Guilin University of Electronic Technology, Guilin 541004, P.R. China

[4] State Key Laboratory of Inorganic Synthesis and Preparative Chemistry, College of Chemistry, Jilin University, Changchun 130012, P.R. China

e-mail: xingyongheng2000@163.com tel: 0411-82156987

Received (in XXX, XXX) Xth XXXXXXXXX 200X, Accepted Xth XXXXXXXXX 200X
First published on the web Xth XXXXXXXXX 200X
DOI: 10.1039/b000000x

Four uranyl complexes $(UO_2)_2(\mu_2\text{-OH})(\mu_3\text{-OH})(his)(CH_3CO_2)$ (his=histidine) (**1**), $[(UO_2)_2(\mu_2\text{-OH})(\mu_3\text{-OH})_2(gly)]\cdot 1.5H_2O$ (gly=glycine) (**2**), $UO_2(CH_3CO_2)(\mu_2\text{-OH})$(2,2'-bipy) (**3**) and $UO_2(CH_3CO_2)_2$(2,2'-bipy) (**4**) were synthesized by the reaction of $UO_2(CH_3CO_2)_2\cdot 2H_2O$ as the metal source, histidine, glycine and 2,2'-bipy as the ligand in aqueous system. They were characterized by elemental analysis, IR, UV-Vis, single crystal X-ray diffraction analysis and thermal gravimetric analysis. The structural analysis reveals that complex **1** exhibits one-demensional chain structure constructed by the building unit $[(UO_2)_4O_{10}(C_6O_2N_3)_2]$, and further extend the chain into 2D supramolecular architectures by hydrogen bonding interactions. For complex **2**, uranyl polyhedrons through edge-sharing to form a 2D wave-like layer and furthermore connected by hydrogen bonding to form a 3D supramolecular structure. Complex **3** is a discrete UO_2-2,2'-bipy compound $UO_2(CH_3CO_2)(OH)$(2,2'-bipy). Complex **4** is also a discrete UO_2-acetic-2,2'-bipy compound $UO_2(CH_3CO_2)_2$(2,2'-bipy) which is similar to complex **3**. The adjacent molecules were respectively connected by the hydrogen bonding to form a 2D supramolecular network for **3** and a 1D superamolecular chain for **4**. In order to extend their functional properties, their photoluminescent characterization and photocatalytic properties were also studied firstly.

Introduction

In recent years, actinide-based complexes have attracted considerable interests in their syntheses and characterization. The chemical reactivity of uranium has been intensively investigated in comparison with those of its neighboring 5f metals in the periodic table. The contribution of the uranium-containing samples can be used as nuclear power[1]. However, it also could seriously damage human health and environment. Recently, what strongly attracted us is that the uranium-organic hybird materials combining the unique characteristics and properties of their organic components with uranyl units to produce diversity in structure, bonding and application. Studies on the design, synthesis, and characterization of uranyl-organic compounds have been keeping on fast development from the viewpoints of the exploration of new materials with attractive and promising applications in wide areas of gas storage, ion exchange, intercalation chemistry, photochemistry and catalysis, etc[2].

To our best knowledge, the coordination chemistry of uranium is dominated by U(VI) in the form of uranyl cation UO_2^{2+} with two typical axial uranyl bonds. Uranyl cation usually exhibits three types of coordination environments in the equatorial plane, which inducing tetragonal, pentagonal, and hexagonal bipyramidal geometries[3]. Until now, a large number of uranyl compounds have been synthesized because of their rich structural diversity. Nevertheless, it is worth to mention that the characteristic of organic ligands play a key role in forming the uranyl complexes with various structure. In the reported literatures, most of the researchers selected carboxylate and heterocyclic ligands to construct uranyl compounds with various structures including clusters[4], chains[5], layers[6] and frameworks[7]. Herein, for purpose of clarity, these uranyl complexes reported by predecessors were mainly classified into four types based on the different style of the ligands: (i) the rigid carboxylate uranyl complexes, such as $UO_2(H_2O)$(1,2-bdc)·$0.32H_2O$, UO_2(1,4-bdc), UO_2(1,3-bdc)[8], (ii) the flexible carboxylate uranyl complexes, such as $UO_2(C_7H_{10}O_4)$, $UO_2(C_8H_{12}O_4)$, $UO_2(C_6H_8O_4)(H_2O)_2$[9], (iii) the N-containing heterocyclic complexes, such as $(UO_2)_2$(2,2'-bpy)(CH_3CO_2)(O)(OH), $UO_2(NO_3)_2$(bpm) (bpm=2,2'-bipyrimidine)[2a, 10], (iv) the uranyl complexes including the carboxylic and N-containing heterocylic ligand, for example: $[(UO_2)_3(L^1)_4(NO_3)_2(H_2O)_2]·2H_2O$ (HL^1=pyridine-2-carboxylic acid)[11]. After careful investigation of the uranyl complexes based on different types of ligands above, it is found that the numerous uranyl complexes including the carboxylic and/or N-containing heterocylic ligand are reported, but study on uranyl complexes with amino acid ligand is rare. With the aim to have a deeper insight of further investigate the influence of this type of ligands on the architectures of uranyl complexes, we choose amino acids as ligand to synthesize uranyl complexes in this article. To our best knowledge, amino acid is not only an important compound of life, but also having essential elements to human body. Amino acids are biologically important organic compounds composed of amine and the carboxylic acid functional groups, which have particular applications in biochemistry. In addition, amino acids have two potential binding sites due to the O-donor and N-donor, which is especially preferable to bond to uranium atom to form a class of crystalline microporous uranyl-organic materials with well-defined channels and rich functionalities. Except for gas uptake and storage properties, uranyl-organic complexes are often considered as efficient heterogeneous photocatalytic activity catalysts candidates because: i) maximum dispersed and uniformly distributed uranyl ions in uranium-based complexes provide numerous potential catalytic centers; ii) highly ordered open channels with well-defined size and shape offer excellent selectivity of substrates; iii) heterogeneous nature of uranium-organic hybird materials facilitates the recovery and reuse of the catalysts. However, many metal-organic frameworks reported to date are not catalytically active due to the coordinative saturation of their metal sites. Therefore exploring desirable active metal centers is very important to achieve framework activity. Uranium-based compounds exhibit versatile physiochemical properties, for example, luminescence[12], photocatalytic performance[13], and photoelectric conversion[4, 14].

In this context, we choose $UO_2(CH_3CO_2)_2·2H_2O$ as a starting materials, histidine and glycine as the ligand, four uranyl complexes $(UO_2)_2$ (μ_2-OH) (μ_3-OH) (his) (CH_3CO_2) (**1**), $[(UO_2)_2(\mu_2\text{-OH})(\mu_3\text{-OH})_2(gly)]·1.5H_2O$ (**2**), $UO_2(CH_3CO_2)(\mu_2\text{-OH})$(2,2'-bipy) (**3**), and $UO_2(CH_3CO_2)_2$(2,2'-bipy) (**4**) have been successfully synthesized. These complexes were characterized by single-crystal X-ray diffraction, IR spectra, UV-vis spectra and XRD analysis, the thermal properties, photocatalytic properties and luminecence of them were also studied.

Experimental Section

Materials. All other chemicals purchased were of reagent grade or better and used without further purification. IR spectra were recorded on a JASCO FT/IR-480 PLUS Fourier Transform spectrometer with pressed KBr pellets in the range 200-4000 cm^{-1}. The elemental analyses for C, H, and N were carried out on a Perkin Elmer 240C automatic analyzer. Thermogravimetric analyses (TG) were performed under atmosphere with a heating rate of 10 ºC/min on a Perkin Elmer Diamond TG/DTA. The luminescence spectra were recorded on a JASCO F-6500 spectrofluorimeter (solid). UV-vis spectra were recorded on JASCO V-570 spectrometer (200-1100 nm, in form of solid sample). X-ray powder diffraction (PXRD) patterns were obtained on a Bruker Advance-D8.

Synthesis. ***Caution!*** *Whereas the uranium oxynitrate hexahydrate ($UO_2(CH_3COO)_2·2H_2O$) used in this study contains depleted U, standard precautions for handling radioactive substances should be followed.*

$(UO_2)_2$ (μ_2-OH) (μ_3-OH) (his) (CH_3CO_2)(1). $UO_2(CH_3CO_2)_2·2H_2O$ (0.1058 g, 0.25 mmol) and histidine (0.0387 g, 0.25 mmol) were dissolved in water (5 ml) and stirred for 4 h at room temperature giving a yellow solution. Then the mixed solution was heated at 80 °C for one day, and yellow crystals were obtained. Yield (based on U): 49.35%. Anal. Calc. For $C_8H_{11}O_{10}N_3U_2$: C, 12.23; H, 1.40; N, 5.35. Found: C, 12.27; H, 1.51; N, 5.32.

$[(UO_2)_2(\mu_2\text{-OH})(\mu_3\text{-OH})_2(gly)]·1.5H_2O$(2).$UO_2(CH_3CO_2)_2·2H_2O$ (0.1058 g，0.25 mmol) and glycine (0.0187 g，0.25 mmol) were dissolved in water (10 ml), and the mixture was stirred at room temperature for 1 h, the yellow solution was obtained. Then the mixed solution was heated at 80 °C for four days, yellow single crystals of **2** for X-ray diffraction analysis were obtained. Yield (based on U): 54.61%. Anal. Calc. For $C_2H_{10}N_2O_{10.5}U_2$: C, 3.40; H, 1.41； N, 3.96. Found: C, 3.41; H, 1.49； N, 3.89.

$UO_2(CH_3CO_2)(\mu_2$-OH)(2,2'-bipy) (**3**). $UO_2(CH_3CO_2)_2·2H_2O$ (0.1058 g, 0.25 mmol), histidine (0.0387 g, 0.25 mmol), 2,2'-bipy (0.0391 g, 0.25 mmol) and H_2O (10 ml) were mixed in a 25ml beaker and stirred for 2 h, then the final reaction mixture was heated at 80 °C for one day, yellow block single crystals of **3** for X-ray diffraction analysis were obtained, but the low yield did not allow for additional chemical characterization. Yield (based on U):

35.06%. Anal. Calc. For $C_{12}H_{12}N_2O_5U$: C, 28.67; H, 2.39; N, 5.57. Found: C, 28.60; H, 2.44; N, 5.53.

$UO_2(CH_3CO_2)_2$(2,2'-bipy) (4). $UO_2(CH_3CO_2)_2 \cdot 2H_2O$ (0.1058 g, 0.25 mmol) , histidine (0.0387 g, 0.25 mmol) and 2,2'-bipy (0.0391 g, 0.25 mmol) were dissolved in deionizer water (15 ml), and stirred for 40 min at room temperature giving a yellow solution. Then the mixed solution was placed at room temperature for one week, yellow single crystals of **4** for X-ray diffraction analysis were obtained. Yield (based on U): 47.07%. Anal. Calc. For $C_{14}H_{14}N_2O_6U$: C, 30.87; H, 2.57; N, 5.14. Found: C, 30.82; H, 2.63; N, 5.07.

X-ray Crystallographic Determination. Suitable single crystals of four complexes were mounted on glass fibers for X-ray measurement, respectively. Reflection data were collected at room temperature on a Bruker AXS SMART APEX II CCD diffractometer with graphite monochromatized Mo Kα radiation (λ=0.71073 Å). All the measured independent reflections ($I > 2\sigma(I)$) were used in the structural analyses, and semi-empirical absorption corrections were applied using SADABS program[15]. Crystal structures were solved by the direct method. All non-hydrogen atoms were refined anisotropically. Hydrogen atoms on carbon and nitrogen were fixed at calculated positions and refined by using a riding model. The hydrogen atom of coordination water molecules were found in difference Fourier map. All calculations were performed using the SHELX-97 program[16]. Crystal data and details of the data collection and the structure refinement are given in Table.1. The selected bond lengths and angles around metal atom of complexes 1-4 are listed in Table.S1-S4.

Results and Discussion

Synthesis: For having a deep insight of further investigate the influence of the amino acids on the architectures of uranyl complexes, we choose $UO_2(CH_3CO_2)_2 \cdot 2H_2O$ as a starting material, histidine and glycine as the ligands. In view of the amino acids with high solubility in water, we choose water as the solvent in the reaction system. Two new uranyl complexes have been synthesized by the reaction of mixing $UO_2(CH_3CO_2)_2 \cdot 2H_2O$, the amino acids and solvent of water, furthermore heating in a pyrex flask at 80 °C for four days or one day. In order to obtain complexes with more complicated structures and dimensions, which have potential applications in functional materials, we try to add 2,2'-bipy to this reaction system as the auxiliary ligand. We expect that both amino acids and 2,2'-bipy could coordinate to uranium atom to get rigid-flexible mixed uranyl complexes as we designed previously. However, the reaction results found that only uranyl-2,2'-bipy complexes were obtained. It is indicated that the coordination capability of 2,2'-bipy is obviously stronger than that of amino acids in this system above.

It is worth to mention that there are some differences in structure between complex **3** and **4**, which may be attribute to the different reaction condition. By the solution method, complex **4** was successfully synthesized at room temperature, while via heating at 80 °C to react for one day, complex **3** was also obtained. The results revealed that the temperature is also a key factor of the reaction to form the complexes, and acetic acid maybe more easily coordinated to uranium atom at room temperature. In addition, complexes **1-4** are all stable at room temperature, and slightly soluble in DMSO and DMF, almost insoluble in water.

Structural Description of Complexes 1-4:

Structure of the complex 1: The asymmetric unit of complex **1** is shown in Fig. 1a. Structural analysis shows that the complex **1** was crystallized in the monoclinic system with *C2/c* space group. The asymmetric unit of **1** consisted of two uranyl cations, one histidine ligand, one two-bridging hydroxyl-oxygen group, one three-bridging hydroxyl-oxygen group and one CH_3COO^- ligand. This uranium atom (U1) coordinated with two oxygen atom (O3, O4) in the axial direction, one oxygen atom (O8) of the CH_3COO^- ligand, one oxygen atom ($O7^{\#1}$) and one nitrogen atom ($N1^{\#1}$) from the histidine ligand, one two-bridging hydroxyl-oxygen atom (O5) and one three-bridging hydroxyl-oxygen atom (O6) in the equatorial plane to form a pentagonal bipyramid polyhedrogen. Similarly, the uranium atom (U2) was seven-coordinated by two oxygen atoms (O1, O2) of the uranyl cation, two oxygen atoms (O10, $O9^{\#2}$) from the histidine ligand and CH_3COO^- group, respectively, and three bridging oxygen atoms (O5, O6, $O6^{\#2}$) to generate a pentagonal bipyramid geometry.

For complex **1**, the four U=O bond distances were 1.794(13), 1.771(14), 1.795(14) and 1.786(14) Å for U1-O3, U1-O4, U2-O1 and U2-O2, respectively. The bond length of U-N was 2.596(15) Å and the distance of $U\text{-}O_{bridging}$ ranged from 2.236(11) to 2.401(11) Å. Additionally, the uranyl ions (U1 and U2) have nearly linear $[O=U=O]^{2+}$ bond angles of 174.0(6) ° and 176.3(6) °. In the structure of complex **1**, two histidine ligand and four uranyl polyhedrons constructed a building $[(UO_2)_4O_{10}(C_6O_2N_3)_2]$ unit via the edge-sharing polyhedral connection (Fig. 1c), in which the histidine adopted terminal coordination mode. One oxygen atom of the carboxylate group from the histidine acted as a bridge to link these units one by one and furthermore formed an infinite 1D chain structure (Fig. 1b). There are three kinds of hydrogen bonds in complex **1**: (i) N—H···O type between the nitrogen atom from the five-number ring of histidine ligand and oxygen of uranyl cation; (ii) N—H···O type between the nitrogen atom from the chain of histidine ligand and oxygen atom of uranyl cation; (iii) C—H···O type between the carbon atom from histidine ligand and oxygen atom uranyl cation. By the hydrogen bonding interaction of (i), the molecules were connected to a 2D network structure along *ab* plane (Fig. 1d). Hydrogen bonding of (ii) linked molecules to form a 2D network structure along *ab* plane (Fig. 1e). By the hydrogen bonding interaction of (i), (ii) and (iii), a 2D supramolecular structure formed (Fig. 1f).

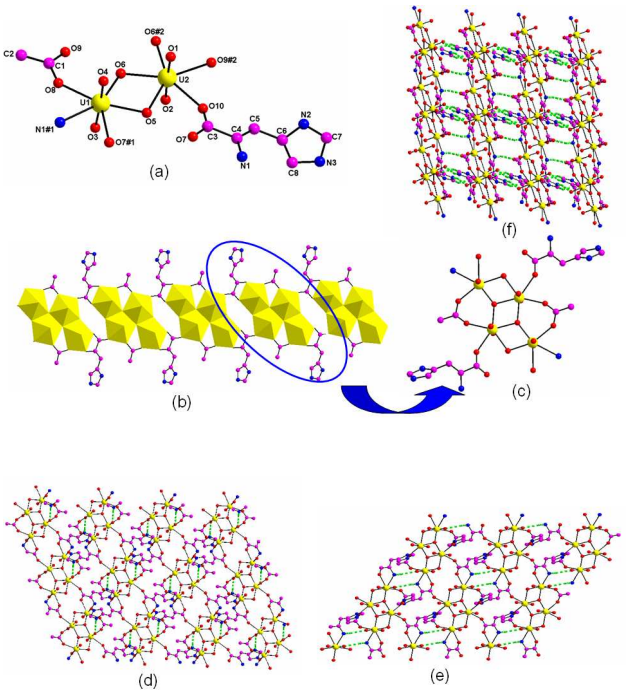

Figure 1. (**a**): The asymmetric unit of complex **1**(Symmetry codes: #1: 3/2-x,1/2-y,1-z; #2: 1-x,1-y,1-z); (**b**): The 1D chain structure of complex **1**; (**c**): The building unit of complex **1**; (**d**): The 2D network structure connected by hydrogen bonding of (i) along *ab* plane of complex **1**; (**e**): The 2D network structure connected by hydrogen bonding of (ii) along *ab* plane of complex **1**; (**f**): The 2D supramolecular structure of complex **1**

Structure of the complex 2: The single-crystal X-ray analysis reveals that complex **2** is crystallized in the monoclinic system with space group *C2/c*. As shown in Fig. 2a, the asymmetric unit of complex **2** consisted of two uranyl cations, one glycine ligand, one two-bridging hydroxyl-oxygen group, two three-bridging hydroxyl-oxygen groups and one and a half lattice water molecule. The U1 was seven-coordinated by two oxygen atoms (O3, O4) in the axial direction, one oxygen atom (O9) from the glycine ligand and four three-bridging hydroxyl-oxygen atoms (O6, $O6^{\#2}$, O7, $O7^{\#4}$) in the equatorial plane to generate a slightly distorted pentagonal bipyramid geometry. U2 adopted the same coordination mode as that of U1. The seven oxygen atoms coordinated with U2 were fromed by two oxygen atoms (O1, O2) from uranyl, one oxygen atom (O8) from the glycine ligand, two three-bridging hydroxyl-oxygen atoms (O6, $O7^{\#5}$) and two two-bridging hydroxyl-oxygen atoms (O5, $O5^{\#1}$). Thus, seven oxygen atoms coordinated to U2 to form a slightly distorted pentagonal bipyramid UO_7 polyhedron configuration. U1 and U2 were connected by two oxygen atoms (O8, O9) from one carboxylate group of glycine and one three-bridging oxygen atom (O6), which furthermore stabilized the structure of complex **2**. In complex **2**, the glycine ligand also adopted terminal coordination mode that similar to complex **1**.

The two uranyl ions U1 and U2 have nearly linear $[O=U=O]^{2+}$ bond angles of 176.5(5) and 175.8(6)°, respectively. The four U=O bond distances were 1.796(12), 1.788(12), 1.781(13) and 1.778(12) Å for U1-O3, U1-O4, U2-O1 and U2-O2, respectively. The bond distances of $U\text{-}O_{glycine}$ were in the range of 2.368(12)-2.474(11) Å. Additional, the bond length of $U\text{-}O_{two\text{-}bridging}$ and $U\text{-}O_{three\text{-}bridging}$ were 2.336(12) and 2.372(11) Å, respectively.

For having a deeply understanding of the structure framework, it would be essential to explore the connection ways of the metal centers and the glycine. In complex **2**, uranyl polyhedrons through edge-sharing to form an infinite 1D chain structure along a axis direction, and the chain was furthermore connected by pentagonal pyramids sharing edge to a 2D wave-like layer (Fig. 2b). As shown in Fig. 2c, it is the 2D wave-like layer of complex **2** along bc plane. In addition, there are five kinds of hydrogen bonds in complex **2**: (i) N−H···O type between the nitrogen atom from glycine and oxygen atom from uranyl cation; (ii) C−H···O type between the carbon atom from glycine and oxygen from carboxyl group of glycine; (iii) C−H ···O type between the carbon atom from glycine ligand and oxygen from uranyl cation; (iv) O−H···O type between the lattice water molecule and the uranyl cation; (v) O−H···N type between the oxygen atom from lattice water molecule and the nitrogen atom from glycine. Hydrogen bonding of (i) linked adjacent asymmetric units to form an infinite 1D supramolecular chain like a zigzag (Fig. 2d). Furthermore, as shown in Fig. 2e, the molecules were connected to a 3D supramolecular structure by the hydrogen interactions of (i), (ii) and (iii). It is interesting that both hydrogen bondings (ii) and (iii) presented a bifurcate connection mode. Additionally, the molecules were furthermore stabilized by the hydrogen bonding interactions of (iv) and (v).

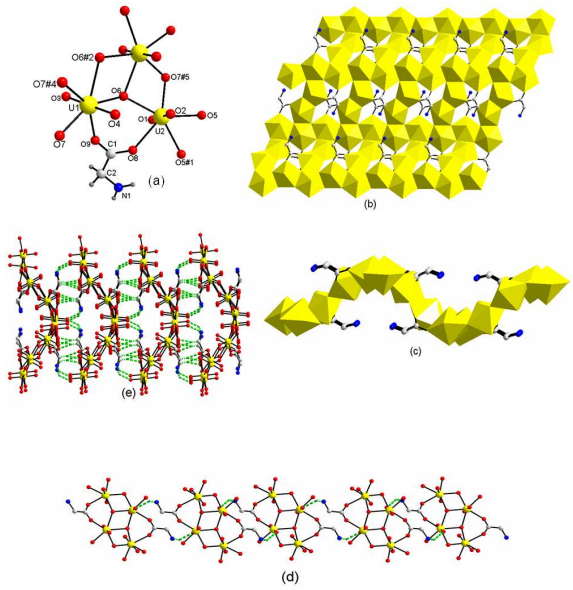

Figure 2. (**a**): The asymmetric unit of complex **2**(the free water molecule has been omitted)(Symmetry codes: #1: 2-x,2-y,1-z; #2: 1-x,y,1/2-z; #4:-x,y,1/2-z; #5: 1+x,y,z); (**b**): The 2D wave-like layer of complex **2**; (**c**): The wave-like layer of complex **2** along *bc* plane; (**d**): The 1D chain structure connected by hydrogen bonding of (i) of complex **2**; (**e**): The 3D supramolecular structure of complex **2**

Structure of the complex 3: The single-crystal X-ray analysis reveals that the complex **3** is crystallized in the orthorhombic system with space group *Pbca*. As shown in Fig. 3a, the asymmetric unit of complex **3** contained one uranyl ion, one 2, 2'-bipy ligand, one two-bridging hydroxyl-oxygen group and one CH_3COO- ligand. The uranium atom coordinated with two oxygen atoms (O1, O2) in the

axial direction, two nitrogen atoms (N1, N2) from one 2,2'-bipy ligand, two two-bridging hydroxyl-oxygen atoms (O3, $O3^{\#1}$) and two oxygen atoms (O4, O5) of carboxylate groups in the equatorial plane to form a hexagonal bipyramid geometrical configuration. The bond lengths of U=O are 1.763(5) and 1.769(5) Å, the length of U-O was in the range of 2.273(6) to 2.484(4) Å and the length of U-N was 2.612(4) and 2.654(5) Å. The uranyl ion has nearly linear $[O=U=O]^{2+}$ bond angle of 174.7(3)° and the bond angle of N-U-N was 61.75(14)°. There were two kinds of hydrogen bonds in complex **3**: (i) C−H···O type between the carbon atom from 2, 2'-bipy ligand and oxygen atom from CH_3COO- group; (ii) C−H···O type between the carbon atom from 2, 2'-bipy ligand and oxygen atom from uranyl cation. Hydrogen bonding of (i) and (ii) linked adjacent asymmetric units to form a 2D supramolecular network structure (Fig. 3b).

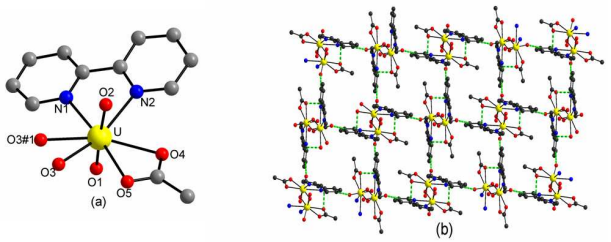

Figure 3. (**a**): The asymmetric unit of complex **3**(Symmetry codes: #1: -x,-y,1-z); (**b**): The 2D supramolecular network connected by hydrogen bonding of (i) and (ii) of complex **3**

Structure of the complex 4: Complex **4** crystallized in the monoclinic system with $P2_1/n$ space group. There was one crystallographically distinct uranyl center, two CH_3COO^- groups and one 2, 2'-bipy ligand in the asymmetric unit (Fig. 4a). The uranyl center was coordinated by two oxygen atoms (O1, O2) in the axial direction, two nitrogen atoms (N1, N2) from one 2,2'-bipy ligand and four oxygen atoms (O3, O4, O5, O6) of carboxylate groups in the equatorial plane, resulting in a distorted hexagonal bipyramid. The U=O lengths were 1.760(3) and 1.755(3) Å, respectively, while the U-O distances in the equatorial plane ranged from 2.437(3) to 2.472(3) Å. The bond lengths of U-N1 and U-N2 were 2.632(4) and 2.643(4) Å, respectively. The uranyl ion has nearly linear $[O=U=O]^{2+}$ bond angle of 179.08(15)°. In addition, the molecule of the complex **4** was linked to form a 1D chain supramolecular structure by the hydrogen bonding interactions of C14−H14C···O2 (3.3781 Å, 174°) (Fig. 4b).

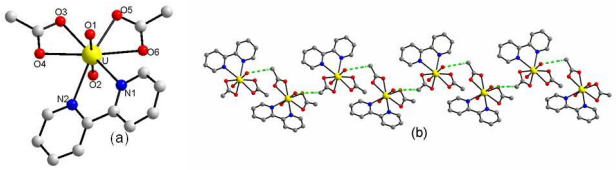

Figure 4. (**a**): The asymmetric unit of complex **4**. (**b**): One-dimensional chain through hydrogen bond of complex **4**

Structural Comparison:

By comparison, the angles of O=U=O of the four complexes are all closed to 180°, which is similar to those reported in the literature. Comparison of corresponding bond lengths and angles of some relevant uranyl complexes with carboxylate ligand is given in Table 2, it is conclusion that the U=O bond length of uranyl complexes with amino acid ligand is slightly longer than those uranyl complexes with the carboxylate ligand, and the angles of O=U=O in those complexes with amino acid ligand is slightly smaller. Moreover, the U-$O_{carboxylate}$ bond lengths of the complexes with histidine ligand are slightly longer than those in uranyl complexes with glycine ligand. In complexes **1**-**4**, the order of the angles of O=U=O is **4** > **2** > **1** > **3**, it should be attributed to the different coordination environments around uranyl groups. As it reported in the literatures, the uranyl complex usually is completed by four to six U-O bonds in the equatorial plane, having the average bond length of 2.28 Å for the hexa-coordinated uranium polyhedra, 2.37 Å for the hepta-coordinated one and 2.47 Å for the octa-coordinated one[17]. Additionally, the coordination environment of uranyl were different in the complexes. For complex **1** and **2**, the uranyl was seven-coordinated to form a pentagonal bipyramid geometric configuration while the uranyl was eight-coordinated to generate a hexagonal bipyramid geometry in complex **3** and **4**. Even though both of histidine and glycine in complexes **1** and **2** adopted terminal coordination mode, the packing fashion and the linking fashion of hydrogen bonding for these complexes were different. In the structure of complex **1**, the building unit $[(UO_2)_4O_{10}(C_6O_2N_3)_2]$ was formed by four uranyl polyhedrons and two histidine ligand, and four uranyl polyhedrons were connected by histidine to form an infinite 1D chain structure. It is worth to mention that the building unit $[(UO_2)_4O_{10}(C_6O_2N_3)_2]$ of complex **1** exhibits an interesting type of linkage. The building unit consists of four pentagonal bipyramids, two of them share two edges and one corner with two adjacent neighbors and the other two have only one edge and one corner in common with the first pair of uranyl centers[17]. The connection nodes between the pentagonal bipyramid all occured in the equatorial plane. Furthermore, the molecular configuration of complex **1** is similar to that of compound $(Hdib)_2[(UO_2)_2O(OH)(siph)]$[18]. In complex **2**, the pentagonal pyramids (UO_7) through edge-sharing to form a 2D wave-like layer, the molecule was furthermore connected by hydrogen bonding to form a 3D supramolecular structure. Complexes **3** and **4** were a discrete UO_2-2, 2'-bipy complexes, and by the hydrogen bonding interactions, the adjacent molecules of complexes **3** and **4** were connected to form a 2D supramolecular network and an infinite 1D supramolecular chain structure, respectively.

IR spectra: For IR spectrum of complex **1** (Fig. S1), the peaks at 3345, 3281, 3142 cm^{-1} should be attributed to the stretching vibration of N-H from the histidine ligand. The characteristic band shown at 3026 cm^{-1} was attributed to the stretching vibration of =C-H. Weak absorptions observed at 2892 and 2863 cm^{-1} are features of the ν_{C-H} vibration modes of $-CH_2-$ within the histidine ligand. The strong peak at 1600 cm^{-1} should be attributed to the asymmetric stretching of COO^- whereas the symmetric peak was observed at 1553 cm^{-1}. The strong bonds appearing in the region of 904-858 cm^{-1} were ascribed to the characteristic absorptions for the asymmetric and symmetric stretching vibrations of bond U=O, which were associated with the structure of complex **1**.

The IR spectrum of complex **2** was shown in Fig. S2, a broad band from 3568 to 3435 cm^{-1} were associated with free water molecules. The peak at 3124 cm^{-1} should be attributed to the stretching vibration of N-H from the ligand. The strong peak at 1569 cm^{-1} should be attributed to the asymmetric stretching of COO^- whereas the symmetric stretching viberation was observed at 1447 cm^{-1}. The asymmetric and symmetric stretching modes of the uranyl cation, range from 912 to 864 cm^{-1}[27], which were associated with the structure of **2**.

The IR spectrum of complex **3** was shown in Fig. S3, the peak at 3414 cm^{-1} was attributed to the stretching vibration of O-H. The

strong bonds appearing in the region of 917-859 cm^{-1} were ascribed to the characteristic absorptions for the asymmetric and symmetric stretching vibrations of bond U=O. The characteristic band shown at 1243, 1012, 766, 710 and 678 cm^{-1} indicated the existence of 2, 2'-bipy ligand, which was associated with the structure of **3**.

The IR spectrum of complex **4** was shown in Fig. S4, the group with peaks at 919 cm^{-1}, 862 cm^{-1} was attributed to the asymmetric and symmetric stretching vibrations of bond U=O[27]. The peaks range from 608 cm^{-1} to 1048 cm^{-1} indicated the existence of 2, 2'-bipy ligand, which were associated with the structure of **4**.

Thermal properties: To examine the thermal stability of the complexes, thermal gravimetric analysis (TG) was carried out at a heating rate of 10 °C/min under the condition of N_2 atmosphere with the temperature range from 20 to 1000 °C (Fig. S5-S8). The TG curve of **1** shows only one stage: the weight loss of 63.58% in the range of 275-305 °C should be attributed to the release of one histidine ligand, one CH_3COO^- group and two bridging oxygen atoms. The final residue is corresponding to UO_3 and some remaining constituent of carbon. The TG curve of **2** is divided into three steps. The first weight loss of 3.90% in the range of 35 to 165 °C should be attributed to one and a half lattice water molecules. The second weight loss occurs in the range of 165-314 °C, with a percentage weight loss of 12.97%, which is ascribed to the release of one coordinated water molecule and one glycine ligand. The last step of decomposition occurred within the range of 314 to 1000°C, which is considered the loss of two bridging oxygen atoms, and the final residue is corresponding to UO_3 and some remaining constituent of carbon. The TG behavior of these complexes is slightly different due to the differences of organic composition in the structures. The TG curve of **3** shows only one stage: the weight loss of 22.17% in the range of 322 to 343 °C is attributed to the release of half 2, 2'-bipy ligand and one CH_3COO^- group. The final residue is corresponding to UO_3 and some remaining constituent of carbon. The TG curve of **4** shows only one stage: the weight loss of 51.79% in the range of 184 to 556 °C is attributed to the release of one 2, 2'-bipy ligand and one CH_3COO^- group. The final residue is corresponding to UO_3 and some remaining constituent of carbon.

XRD analysis: The powder X-ray diffraction data of the complexes **1**-**4** were obtained and compared with the corresponding simulated single-crystal diffraction data (Fig. S9-S12). The phase of the corresponding complex is considered as purities owning to the agreement of the peak positions. The different intensity may be due to the preferred orientation of the powder samples.

Photoluminescent properties: The fluorescence on uranyl compounds is currently a significant attention in the development of fluorescent materials. The uranyl ion is a fluorescent centre. The luminescence spectra of uranyl compounds are located in the visible region (480-600nm)[28]. It is necessary to have an investigation of the photoluminescence with regard to the uranyl compounds. The structure and intensity of uranyl luminescence spectra depend on the bonding, symmetry and the local environment of UO_2^{2+}[29]. In general, fluorescence of uranyl complexes typically has a characteristic six peaks relating to the $S_{11}\rightarrow S_{00}$ and $S_{10}\rightarrow S_{0v}$ electronic transitions, where v=0-4[30]. But the luminescent properties regarding complex **1** were studied at the excitation wavelength of 400 nm and only three peaks (471, 526, 547 nm) were presented in Fig. 5a. The luminescent properties regarding complex **3** was studied at the excitation wavelength of 364 nm and three peaks (418, 516, 531 nm) were presented in Fig. 5c. This should be attributed to the overlap of the energy level after coordination with the organic ligand, leading to the change of electronic configuration. Similarly, complex **4** was studied at the excitation wavelength of 368 nm and only two peaks (529 nm, 542 nm) were presented in Fig. 5b. The photoluminescent spectra of the three complexes both exhibit a broad peak, which should due to presence of organic conjugating system leading to the overlap of the energy level. However, according to the experimental results, it is found that the photoluminescent peak of complex **2** was not observed, this phenomenon of fluorescence quenching may be attributed to that the excitation energy of glycine ligand is not match with the excitation energy of uranyl. To the best of our knowledge, not all uranyl complexes exhibit luminescence of UO_2^{2+} cations. This is a common phenomenon because many factors are relevant to the luminescent property, such as size and quality of the crystal, disorder within the equatorial plane of the uranyl group, and so on[31].

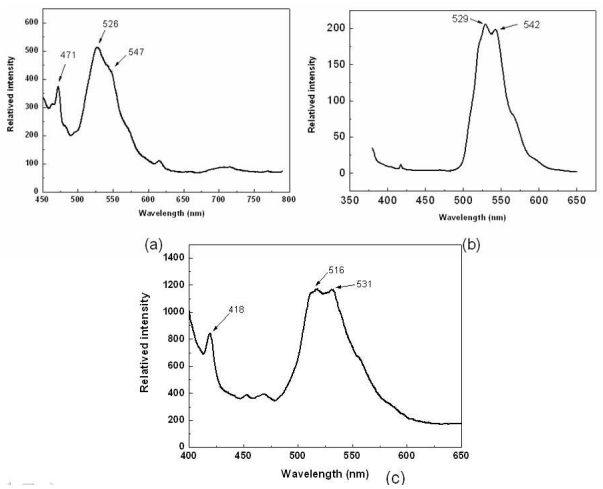

Figure 5. (**a**): The photoluminescent spectrum of the complex **1**(the excitation wavelength is 400 nm); (**b**): The photoluminescent spectrum of the complex **4**(the excitation wavelength is 368 nm); (**c**): The photoluminescent spectrum of the complex **3**(the excitation wavelength is 364 nm)

UV-vis spectra: The diffuse reflectance of UV-vis spectra of complexes **1**-**4** were shown in Fig. S13-S16. For complex **1**, there are three peaks presented in the spectroscopy, the peaks at 210 nm should be attributed to the electronic transition of the ligand, the peak at 312 nm, 442 nm should be attributed to the electronic transition between the U=O double bond[32,33]. Similarly, the spectroscopy of complex **2** occurred three peaks at 209, 319 and 437 nm, which were also attributed to the typical absorption peaks of $(UO_2)^{2+}$. For complexes **3** and **4**, three peaks (214 nm, 323 nm, 435 nm) and (256 nm, 331 nm, 435 nm) occurred in the UV-vis spectrum respectively, which is associated to the typical absorption of uranyl cation. It worth to mention, by comparing with complex **1**-**4**, we found that the shape and position of the peaks are almost similar, only the absorption intensities of complex **3** and **4** were slightly weaker than complex **1** and **2**, which nearly due to the different type of the ligands.

Photocatalytic Performance: Photocatalysts have attracted much attention due to their potential applications in purifying waste water and air by thoroughly decomposing organic compounds[34]. Among these photocatalysts, the kinds of uranyl-contained complexes were extraordinary important because of the thoroughly decomposing of organic polluction which completed by the uranyl double bond[35]. As we all know, methyl blue, methyl orange and rhodamine B (RhB) as the dyes have been widely used in textile, printing, paper and pharmaceutical industry, but causing serious pollution to the environment at the same time[36]. In this work, we selected methyl

blue and rhodamine B as the model compound of organic pollutant to investigate the degradation efficiency using complex **1** as catalyst. With the aim to have a deep insight of further investigate of the degradation efficiency of the dye, we also studied the degradation efficiency under the irradiation of UV and visible light, respectively. During the degradation process, we used a 18 W Hg lamp as UV light source and a 125 W Xe lamp as the visible light source. The distance between the reaction vessel and the light source was all 15 cm. And during the process of the decomposing reaction, a UV-1000 spectrophotometer was used to monitor the reaction under the specific given wavelength. To rule out the possibility that the photocatalytic activity of the complex arises from molecular or oligomeric species formed through dissolution of the solid samples in the photocatalytic reaction systems, control experiments were conducted. We subjected the catalysts to UV and visible light and continuous stirring in water for 3h, and tested the photocatalytic activity of the solution after filtering off the solid materials. No catalytic activity was observed for the solution.

In this work, we take complex **1** as the example to illustrate the degradation efficiency intail. Firstly, the photodegradation activity was tested by using a solution of rhodamine B (RhB) as a target pollutant for degradation experiments. For comparison, the degradation reaction was also tested under UV and visible light, respectively. As it is shown in Fig.6a, in the presence of complex **1,** only a very small decrease in intensity for the characteristic absorption of RhB was observed under visible light irradiation. However, under the irradiation of UV light (Fig.6b), the decrease intensity of absorption was larger than that of under visible light irradiation. As it is shown in Fig.8b, for comparison, the self-degradation of RhB was also assessed under the same experimental conditions. It obviously revealed that without the solid catalyst in the reaction system, the RhB hardly degraded in 3 h of irradiation under UV and visible light, suggesting that the solution contains no photocatalytically active species. However, in the presence of complex **1**, the RhB in the aqueous solution is degraded 8.61% under the irradiation of UV light and 1.64% under the irradiation of visible light in the early 30 min. The slope of the curves (Fig.8b) reflected that the degradation efficiency of the solution under UV light was much better than that under visible light. After degraded the RhB solution in the presence of complex **1** for 3 h under UV light, the degradation rate of it was nearly 17.48%. These results suggest that complex **1** may be not a very good candidate for photocatalytic degradation of RhB.

In addition, we also selected another kind of dye methylene blue as model compound of organic pollutant to investigate the degradation efficiency using complex **1** as catalyst. The absorption spectra of methylene blue solution during the photodegradation reaction under the visible and UV light were shown in Fig.7. Under the irradiation of UV light, the decrease intensity of absorption was remarkable larger than that of under visible light irradiation. As shown in Fig.8a, in the presence of complex **1**, the methylene blue solution is degraded 40.40% in 180 min under visible light and degraded 54.89% under the UV light irradiation. Above all, it revealed that the degradation efficiency of methylene blue solution is much better than that of RhB solution in the presence of complex **1**. These results suggest that complex **1** exhibit high photocatalytic activities under UV and visible light irradiation for methylene blue.

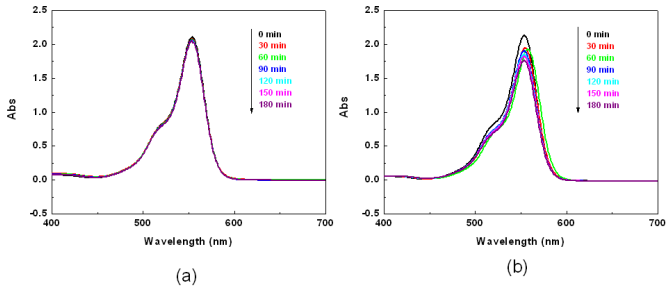

Figure 6. Absorption spectra of rhodamine B (RhB) solution during the photodegradation reaction under the irradiation of (a) visible light and (b) UV light with the use of complex **1**

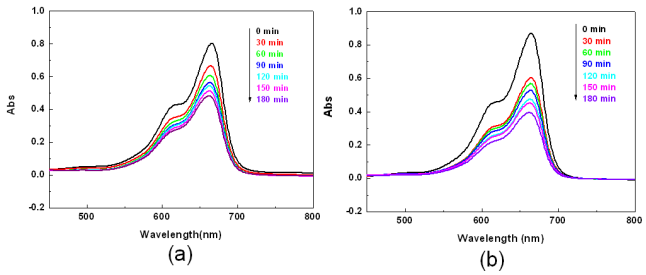

Figure 7. Absorption spectra of methylene blue solution during the photodegradation reaction under the irradiation of (a) visible light and (b) UV light with the use of complex **1**

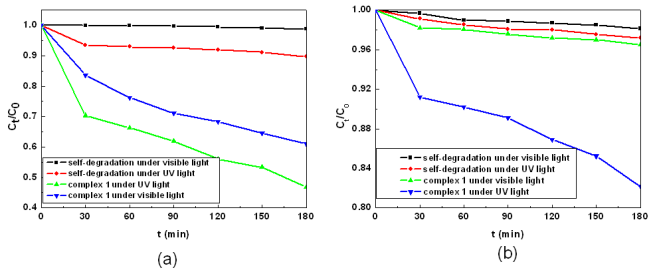

Figure 8. (a): Self-degradation and photocatalytic decomposition of methylene blue solution with the use of complex **1** under UV and visible light; (**b**): Self-degradation and photocatalytic decomposition of rhodamine B (RhB) solution with the use of complex **1** under UV and visible light

For comparison, we also tested the degradation efficiency of complexes **2-4** by using methylene blue as a target pollutant for degradation experiments. For complex **2**, the absorption spectra of methylene blue solution during the photodegradation reaction under the visible and UV light were shown in Fig.S17-18. The self-degradation and photocatalytic decomposition of methylene blue solution with the use of complex **2** under UV and visible light are shown in Fig.S19. The degradation effciency of methylene blue in the presence of complex **2** under visible light was a little better than under UV light, but the methylene blue solution is degraded 23.6% in the early 30 min under visible light and degraded 25.5% under UV light. The absorption spectra of methylene blue solution during the photodegradation reaction of complex **3** under the

visible and UV light were shown in Fig.S20-21. As shown in Fig.S22, the slope of the curves reflected that the degradation efficiency of the solution under UV light was much better than that under visible light in 120 min, however, after degraded the methylene blue solution in the presence of complex **3** for 3 h under UV light and visible light, the degradation rate of it was 32.5% and 35.0%, respectively. The absorption spectra of methylene blue solution during the photodegradation reaction of complex **4** under the visible and UV light were shown in Fig.S23-24, the absorption peaks decreased obviously under visible light, but as shown in Fig.S25, after degraded the methylene blue solution in the presence of complex **4** for 3 h under visible light, the degradation rate of it was nearly 20.3%. Based on analysis above, it is conclusion that the degradation eficiency of complexes **1** and **2** was much better than complexes **3** and **4**. To our best knowledge, the uranyl-contained complexes could degrade the organic pollutions mainly duo to the uranyl double bond. Among complexes **1**-**4**, the high percentage composition of uranium in complexes results in the high degradation efficiency.

The photochemistry of uranyl compounds dates back to the early 1800s. Since then, their photochemistry, especially photocatalytic performance has been studied extensively. Generally, two mechanisms have been proposed for the photocatalytic reactions involving U^{VI} species, that is, hydrogen abstraction and electron transfer (Fig.9)[37]. Electron may be promoted from the HOMO to the LUMO under photoexcitation, the empty uranium orbitals generating excited $*UO_2^{2+}$ species. To our best knowledge, the excited electron in the LUMO is not stable, it may be return to the HOMO. However, the electron from organic molecules (such as RhB) may be abstracted by the $*UO_2^{2+}$ species to form the intermediates. So the HOMO is occupied by the electron from the guest molecules, and the excited electron would remain in the LUMO until they captured by O_2 in the solution, generating highly active peroxide anions. The peroxide anions furthermore oxidize and decompose the organic intermediates in the solution, leading to complete degradation of the organic substances[38].

As illustrated previously, RhB photodegradation in the presence of uranyl photocatalysts also might adopted an abstraction-de-ethylation process, once having reached the photoexcited uranyl centers, the RhB molecules begin to decompose with hydrogen abstraction and then the transitional active complex can be formed. Thus, one α-hydrogen atom of the methylene group bonded to the electron withdrawing nitrogen atom of RhB, which associated to uranyl species, and furthermore cracked to small organic acids and CO_2[24, 39]. The photocatalytic reaction mechanism of methylene blue in the presence of uranyl complex is similar to that of RhB, which also adopted the hydrogen abstraction mechanism.

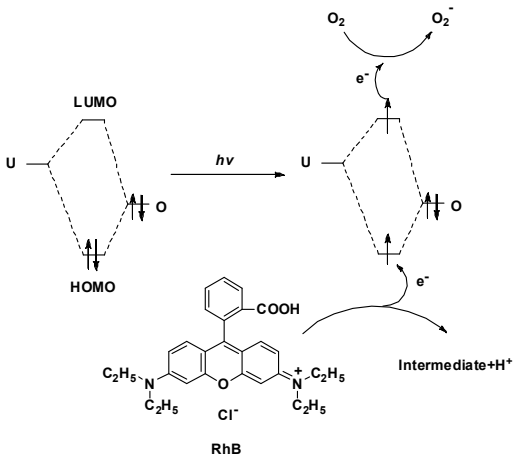

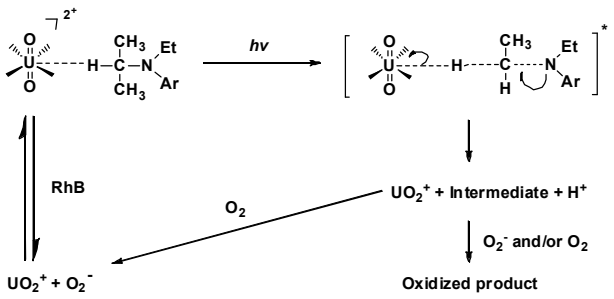

Figure 9. The photocatalytic reaction mechanism of RhB in the presence of uranyl complex

Conclusion

In summary, we have synthesized four uranyl complexes by using histidine, glycine and 2, 2'-bipy as the ligand. Complex **1** features a 1D structure containing four uranyl polyhedrogens as the building unit connected by histidine ligand. Complex **2** is a 2D wave-like layer structure constructed of UO_7 polyhedra and glycine ligand. Complexes **3** and **4** are a discrete molecule, by the hydrogen bonding interactions, the adjacent molecules of complexes **3** and **4** were connected to form a 2D supramolecular network and an infinite 1D supramolecular chain structure, respectively. In addition, the XRD analysis indicating that the bulk products obtained are homogenous in nature. The thermal stability and fluorescence properties were also studied, and the results showed that the complexes have good thermal stability and fluorescence property. Photoluminescent studies reveal those complexes **1**, **3** and **4** display characteristic emissions of uranyl centers. They seem to be good candidates for biological fluorescence materials. Complex **1-4** also exhibit photocatalytic property under UV and visible light irradiation, and complexes **1-3** degrade methylene blue efficiently. This work enriches the structure diversity of uranyl complexes and demonstrates the progress of construction of new uranyl complexes by amino acids ligand. It is believed that, with the further understanding of the uranyl complexes, more physicochemical properties of it will be revealed.

Supporting information paragraph. The selected bond lengths and angles for complexes **1-4** are listed in Tables S1-S4. Their hydrogen bonds are shown in Table S5. Infrared spectra and TG curves of complexes **1-4** are shown in Figs.S1-S4 and Fig.S5-S8. Fig.S9-S12 and Fig.S13-S16 have presented the PXRD patterns and UV-vis spectra of the complexes **1-4**, respectively. Figs.S17-S19 has presented the degradation efficiency of complex **2**. The degradation efficiency of complexes **3** and **4** are shown in Figs.S20-S22 and Figs.S23-S25, respectively. Copies of this information may be obtained free of charge, by quoting the publication citation and deposition numbers CCDC 1008960 for (**3**), 1008961 for (**1**), 1008962 for (**4**) and 1008963 for (**2**) from the Director, CCDC, 12 Union Road. Cambridge, CB2 1EZ, UK (fax+44-1223-336033; e-mail: deposit@ccdc.cam.ac.uk or http://www.ccdc.cam.ac.uk).

Acknowledgements. This work was supported by the grants of the National Natural Science Foundation of China (Grant No. 21071071, 21371086). Guangxi Key Laboratory of Information Materials, Guilin University of ElectronicTechnology, P. R. China (Project No. 1210908-06-K) and State key Laboratory of Inorgnic Synthesis and Preparative Chemistry, College of Chemistry, Jilin University, Changchun 130012, P. R. China (Grant No. 2013-05) for the financial assistance.

Keywords: Uranyl complexes • Histidine • Glycine • Crystal structure • Photocatalytic property

Table 1 Crystallographic data for complexes **1**–**4**

Complex	**1**	**2**	**3**	**4**
Formula	$C_8H_{10}N_3O_{10}U_2$	$C_2H_{10}NO_{10.5}U_2$	$C_{12}H_{12}N_2O_5U$	$C_{14}H_{14}N_2O_6U$
M (g · mol^{-1})	784.25	692.17	502.27	544.30
Crystal system	Monoclinic	Monoclinic	Orthorhombic	Monoclinic
Space group	*C2/c*	*C2/c*	*Pbca*	$P2_1/n$
a (Å)	17.5227(16)	7.2325(16)	11.5887(3)	7.9487(5)
b (Å)	11.7243(10)	16.469(4)	13.7676(4)	19.0021(11)
c (Å)	16.7131(15)	17.315(4)	16.8921(5)	10.5863(6)
α (°)	90	90	90	90
β (°)	112.255(2)	100.814(3)	90	95.6450(10)
γ (°)	90	90	90	90
V (Å^3)	3177.8(5)	2025.9(8)	2695.11(13)	1591.22(16)
Z	8	8	8	4
D_{calc}	3.278	4.539	2.476	2.272
Crystal size (mm)	0.31× 0.20 × 0.18	0.23 × 0.14 × 0.12	0.40 × 0.26 × 0.18	0.17 × 0.21 × 0.11
F(000)	2744	2376	1840	1008
μ(Mo-Kα)/ mm^{-1}	20.412	31.982	12.065	10.232
Reflections collected	9773	5702	9893	9876
Independent reflections ($I > 2\sigma(I)$)	3896(2987)	2396(1608)	2651(2033)	3893(2978)
Parameters	209	141	183	210
Δ(ρ) (e Å^{-3})	1.770 and -2.993	2.498 and -2.506	0.887 and -0.942	0.712 and -0.850
Goodness of fit	1.049	1.004	1.038	0.989
R_1[a]	0.0609 (0.0845)b	0.0506 (0.0872)b	0.0294 (0.0462)b	0.0283 (0.0459)b
wR_2[a]	0.1731 (0.1850)b	0.0946 (0.1088)b	0.0566 (0.0620)b	0.0615 (0.0690)b

[a]$R = \Sigma||Fo| - |Fc|| / \Sigma|Fo|$, $wR_2 = [\Sigma(w(Fo^2 - Fc^2)^2 / [\Sigma(w(Fo^2)^2)^{1/2}$; $[Fo > 4\sigma(Fo)]$.

[b]Based on all data.

Table 2 The relevant bond lengths (Å) and angles (°) of uranyl complexes

Complex	U=O (Å)	U-$O_{carboxylate}$ (Å)	O-U-O (°)	Ref
α-$[(UO_2)_2(C_2O_4)(OH)_2(H_2O)_2]$	1.764(2)	2.440(11)	177.4(9)	[19]
β-$[(UO_2)_2(C_2O_4)(OH)_2(H_2O)_2]$	1.760(2)	2.481(7)	178.8(3)	[19]
$[(UO_2)_2(C_2O_4)(OH)_2(H_2O)_2]\cdot H_2O$	1.770(6)	2.471(7)	178.9(18)	[19]
$UO_2(HL^1)$	1.732(8)	2.376(10)	179.2(14)	[20]
$(UO_2)_3(H_2O)_2L^2$	1.725(11)	2.426(2)	178.8(8)	[20]
$UO_2(tci)(C_3H_5N_2)\cdot H_2O$	1.768(4)	2.461(2)	178.9(6)	[21]
$[UO_2(L^1)(H_2O)]\cdot 3H_2O$	1.756(18)	2.370(8)	176.4(6)	[22]
$[UO_2(L^1)(DMF)]\cdot 0.5H_2O$	1.758(11)	2.378(5)	179.1(9)	[22]
$[UO_2(L^1)(H_2L^1)]\cdot H_2O$	1.763(5)	2.364(19)	175.9(17)	[22]
$[(UO_2)_8(L_{12}H_8)]\cdot 12H_2O$	1.742(5)	2.485(10)	178.1(13)	[23]
$(UO_2)_2(NDC)_2(2,2\text{-bipy})_2$	1.770(10)	2.466(13)	178.4(9)	[24]
$UO_2(4,4\text{-bpdc})$	1.748(10)	2.287(14)	180.0(2)	[25]
$UO_2(1,3\text{-bdc})$	1.759(8)	2.315(5)	180.0(2)	[25]
$[(UO_2)_3(Gly)_2(O)_2(OH)_2](H_2O)_6$	1.785(5)	2.425(9)	175.1(7)	[26]
$[(UO_2)_5(Gly)_4(O)_3(OH)_3](NO_3)(H_2O)_{12}$	1.794(16)	2.437(10)	175.7(11)	[26]
$[(UO_2)_3(Ala)_2O(OH)_3](NO_3)(H_2O)_3$	1.777(11)	2.395(4)	177.6(11)	[26]
$(UO_2)_2(\mu_2\text{-OH})(\mu_3\text{-OH})(his)(CH_3CO_2)$	1.786(13)	2.492(2)	175.2(19)	this work
$[(UO_2)_2(\mu_2\text{-OH})(\mu_3\text{-OH})_2(gly)]\cdot 1.5H_2O$	1.785(5)	2.421(9)	176.1(19)	this work

[1] (a) A. E. V. Gorden, J. Xu, N. K. Raymond, P. Durbin, Chem. Rev., 2003, **103**, 4207-4282; (b) R. C. Ewing, Can. Mineral., 2001, **39**, 697-715; (c) P. Prapaipong, E. L. Shock, C. M. Koretsky, Geochim. Cosmochim. Acta., 1999, **63**, 2547-2577; (d) W. T. Yang, S. Dang, H. Wang, T. Tian, Q. J. Pan, Z. M. Sun, Inorg. Chem., 2013, **52**, 12394-12402.

[2] (a) P. O. Adelani, P. C. Burns, Inorg. Chem., 2012, **51**, 11177-11183; (b) A. N. Alsobrook, B. G. Hauser, J. T. Hupp, E. V. Alekseev, W. Depmeier, T. E. Albrecht-Schmitt, Chem. Commun., 2010, **46**, 9167-9169; (c) P. O. Adelani, T. E. Albrecht-Schmitt, Inorg. Chem., 2011, **50**, 12184-12191; (d) C. L. Cahill, D. T. de Lill, M. Frisch, CrystEngComm., 2007, **9**, 15-26.

[3] (a) H. Y. Wu, W. T. Yang, Z. M. Sun, Cryst. Growth Des., 2012, **12**, 4669-4675; (b) P. C. Burns, M. L. Miller, R. C. Ewing, Can. Mineral., 1996, **34**, 845-880; (c) P. C. Burns, Can. Mineral., 2005, **43**, 1839-1894.

[4] Z. T. Yu, G. H. Li, Y. S. Jiang, J. J. Xu, J. S. Chen, Dalton Trans., 2003, 4219-4220.

[5] P. Thuery, Cryst. Growth Des., 2011, **11**, 347-355.

[6] (a) K. E. Knope, C. L. Cahill, Inorg. Chem., 2009, **48**, 6845-6851; (b) A. T. Kerr, C. L. Cahill, Cryst. Growth Des., 2011, **11**, 5634-5641; (c) P. Thuery, CrystEngComm., 2009, **11**, 232-234.

[7] (a) L. A. Borkowski, C. L. Cahill, Inorg. Chem., 2003, **42**, 7041-7045; (b) J. Lhoste, N. Henry, P. Roussel, T. Loiseau, F. Abraham, Dalton Trans., 2011, **40**, 2422-2424.

[8] (a) I. Mihalcea, N. Henry, T. Loiseau, Cryst. Growth Des., 2011, **11**, 1940-1947; (b) I. Mihalcea, N. Henry, T. Bousquet, C. Volkringer, T. Loiseau, Cryst. Growth Des., 2012, **12**, 4641-4648.

[9] L. A. Borkowski, C. L. Cahill, Cryst. Growth Des., 2006, **6**, 2241-2247.

[10] G. Zucchi, O. Maury, P. Thuery, Chem. Eur. J., 2009, **15**, 9686-9696.

[11] P. R. Silverwood, D. Collison, F. R. Livens, R. L. Beddoes, R. J. Taylor, J. Alloys Compd., 1998, **180**, 271-273.

[12] C. Volkringer, N. Henry, S. Grandjean, T. Loiseau, J. Am. Chem. Soc., 2012, **134**, 1275-1283.

[13] Z. T. Yu, Z. L. Liao, Y. S. Jiang, G. H. Li, J. S. Chen, Chem. Eur. J., 2005, **11**, 2642-2650.

[14] W. Chen, H. M. Yuan, J. Y. Wang, Z. Y. Liu, J. J. Xu, M. Yang J. S. Chen, J. Am. Chem. Soc., 2003, **125**, 9266-9267.

[15] G. M. Sheldrick SADABS, Program for Empirical Absorption Correction for Area Detector Data, University of Göttingen: Göttingen, Germany, 1996.

[16] G. M. Sheldrick, SHELXS-97, Program for Crystal Structure Refinement, University of Göttingen: Göttingen, Germany, 1997.

[17] T. Loiseau, I. Mihalcea, N. Henry, C. Volkringer, Coord. Chem. Rev., 2013, **266**, 69-109.

[18] W. Yang, T. Tian, H. Y. Wu, Q. J. Pan, S. Dang, Z. M. Sun, Inorg. Chem., 2013, **52**, 2736-2743.

[19] L. Duvieubourg, G. Nowogrocki, F. Abraham, J. Solid State Chem., 2005, **178**, 3437-3444.

[20] H. Y. Wu, R. X. Wang, W. T. Yang, Z. M. Sun, Inorg. Chem., 2012, **51**, 3103- 3107.

[21] L. L. Liang, Y. G. Cai, N. S. Weng, R. L. Zhang, J. S. Zhao, Inorg. Chem. Commun., 2009, **12**, 86-88.

[22] P. Thuery, B. Masci, CrystEngComm., 2012, **14**, 131-137.

[23] P. Thuery, Cryst. Growth Des., 2009, **9**, 4592-4594.

[24] Z. L. Liao, G. D. Li, M. H. Bi, J. S. Chen, Inorg. Chem., 2008, **47**, 4844-4853.

[25] I. Mihalcea, N. Henry, T. Bousquet, T. Loiseau, Cryst. Growth Des., 2012, **12**, 4641-4648.

[26] J. Groot, K. Gojdas, D. K. Unruh, T. Z. Forbes, Cryst. Growth Des., 2014, **14**, 1357-1365.

[27] (a) M. B. Doran, A. J. Norquist, Chem. Mater., 2003, **15**, 1449-1455; (b) A. Mer, S. Obbade, M. Rivenet, C. Renard, F. Abraham, J. Solid State Chem., 2012, **185**, 180-186.

[28] J. T. Bell, R. E. Biggers, J. Mol. Spectr., 1968, **25**, 312-329.

[29] (a) Z. Hnatejko, S. Lis, P. Starynowicz, Z. Stryła, Polyhedron., 2011, **30**, 880-885; (b) R. G. Denning, Struct.Bond., 1992, **79**, 215-276; (c) G. Meinrath, J. Radioanal, Nucl. Chem., 1997, **224**, 119; (d) T. Arnold, N. Baumann, Spectrochim. Acta, Part A., 2009, **71**, 1964-1968; (e) I. Billard, E. Ansoborlo, K. Apperson, S. Arpigny, A. E. Azehna, D. Birch, Appl. Spectrosc., 2003, **57**, 1025-1036; (f) I. Lampe, D. Schultze, F. Zygalsky, Polym. Degrad. Stab., 2001, **73**, 87-92.
[30] (a) A. B. Lauren, L. C. Christopher, Cryst. Growth Des., 2006, **6**, 2248-2259; (b) A. B. Lauren, L. C. Christopher, Cryst. Growth Des., 2006, **6**, 2241-2247; (c) A. Brachmann, G. Geipel, G. Bernhard, H. Nitsche, Radiochim. Acta., 2002, **90**, 147-149.
[31] (a) P. O. Adelani, T. E. Albrecht-Schmitt, Cryst. Growth Des., 2011, **11**, 4227-4237; (b) W. T. Yang, S. Dang, H. Wang, Z. M. Sun, Inorg. Chem., 2013, **52**, 12394-12402.
[32] (a) M. Frisch, C. L. Cahill, Dalton Trans., 2005, 1518-1523; (b) R. C. Severance, S. A. Vaughn, M. D. Smith, Solid State Sciences., 2011, **13**, 1344-1353; (c) V. A. Volkovich, T. R. Griffiths, D. J. Fray, R. C. Thied, Phys. Chem. Chem. Phys., 2001, **3**, 5182-5191; (d) P. M. Almond, T. E. Albrecht-Schmitt, Inorg. Chem., 2002, **41**, 1177-1183.
[33] (a) P. M. Cantos, M. Frisch, C. L. Cahill, Inorg. Chem. Commun., 2010, **13**, 1036-1039; (b) H. G. Brittain, D. L. Perry, J. Phys. Chem., 1981, **85**, 3073-3078.; (c) R. S. Addleman, M. Carrott, C. M. Wai, T. E. Carleson, B. W. Wenclawiak, Anal. Chem., 2001, **73**, 1112-1119; (d) J. Huang, X. Wang, A. J. Jacobson, J. Mater. Chem., 2003, **13**, 191-196; (e) H. Kunkely, A. Vogler, Z. Naturforsch. B., 2002, **57**, 301-304.
[34] (a) B. Liu, Z. T. Yu, J. Yang, H. Wu, Y. Y. Liu, J. F. Ma, Inorg. Chem., 2011, **50**, 8967-8972; (b) H. X. Li, X. Y. Zhang, Y. N. Huo, J. Zhu, Environ. Sci. Technol., 2007, **41**, 4410-4414.
[35] M. Sarakha, M. Bolte, H. D. Burrows, J. Photochem. Photobiol. A., 1997, **107**, 101-106.
[36] (a) J. C. Geng, L. Qin, X. Du, S. L. Xiao, G. H. Cui, Z. Anorg. Allg.Chem., 2012, **638**, 1233-1238; (b) E. Haque, J. E. Lee, I. T. Jang, Y. K. Hwang, J. Chang, J. Jegal, S. H. Jhung, J. Hazard. Mater., 2010, **181**, 535-542; (c) L. Qin, S. L. Xiao, P. J. Ma, G. H. Cui, Transit. Met. Chem., 2013, **38**, 627-633.
[37] H. D. Burrows, T. J. Kemp, Chem. Soc. Rev., 1974, **3**, 139-165.
[38] (a) K. X. Wang, J. S. Chen, Acc. Chem. Res., 2011, **44**, 531-540; (b) M. J. Sarsfield, H. Steele, M. Helliwell, S. J. Teat, Dalton Trans., 2003, 3443-3449; (c) V. C. Williams, M. Muller, M. A. Leech, R. G. Denning, M. L. H. Green, Inorg. Chem., 2000, **39**, 2538-2541; (d) R. Nakamura, Y. Nakato, J. Am. Chem. Soc., 2004, **126**, 1290-1298.
[39] Y. Xia, K. X. Wang, J. S. Chen, Inorg. Chem. Commun., 2010, **13**, 1542-1547.

Only Graphic Abstract content

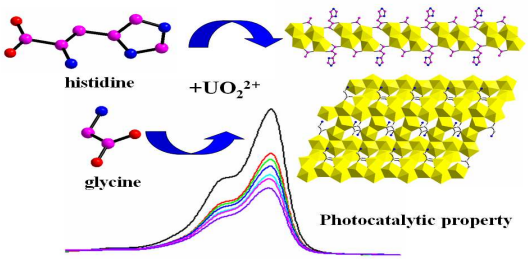

We have synthesized four new uranyl complexes, their photoluminescent characterization and photocatalytic properties were studied in detail.